Plant Physiol. (1996) 111: 1281–1292

Membrane-Delimited Phosphorylation Enables the Activation of the Outward-Rectifying K Channels in Motor Cell Protoplasts of *Samanea saman*[1]

Nava Moran*

Department of Neurobiology, Weizmann Institute, Rehovot 76100, Israel

Outward-rectifying K channels activated by membrane depolarization (K_{out} or K_D channels) control K^+ efflux from plant cells. To find out to what extent phosphorylation is required for the activity of these channels, the patch-clamp method was applied to protoplasts from the legume *Samanea saman* in both whole-cell and isolated-patch configurations. In the absence of either Mg^{2+} or ATP in the "cytosolic" solution, the K_D channel activity declined completely within 15 min. This decline could be reversed in excised, inside-out patches by restoring MgATP (1 mM) to the cytoplasmic side of the membrane. Mg^{2+} (1 mM) plus 5′-adenylylimidodiphosphate (1 mM), a nonhydrolyzable ATP analog, did not substitute for ATP. Mg^{2+} (1 mM) plus adenosine 5′-*O*-(3-thiotriphosphate) (25 to <100 μM), an irreversibly thiophosphorylating ATP analog, sustained channel activity irreversibly. 1-(5-Isoquinolinesulphonyl)-2-methylpiperazine (100 μM), a broad-range kinase inhibitor, blocked the activity of K_D channels in the presence of MgATP. These results strongly suggest that the activation of the outward-rectifying K channels by depolarization depends critically on phosphorylation by a kinase tightly associated with the K_D channel.

Protein phosphorylation is a key step in transduction cascades, from signals to biological responses. Various ion channels in animal cell membranes are among the target phosphoproteins (see recent review by Levitan, 1994, and refs. therein). In plants, phosphorylation/dephosphorylation are also recognized as regulators of ion transport (Zocchi, 1985; Schaller and Sussmann, 1988; Shiina et al., 1988; Martiny-Baron et al., 1992; Roberts and Harmon, 1992; Luan et al., 1993; Sussman, 1994; Armstrong et al., 1995; Schmidt et al., 1995). Recent work on the K channels in guard cells and mesophyll cells of *Vicia faba* and in tobacco guard cells implicated the activities of homologs of protein phosphatase PP2B in the regulation of the inward-rectifyingK channel (Luan et al., 1993) and of protein phosphatases PP1, PP2A, and PP2C in the regulation of the outward-rectifying K channels (Li et al., 1994a; Thiel and Blatt, 1994; Armstrong et al., 1995). The involvement of protein phosphatases suggests that these channels are regulated by protein kinases (Cohen, 1992).

It follows that cAMP, probably acting via a protein kinase A, up-regulated outward K^+ currents in the *V. faba* mesophyll cells (Li et al., 1994b). Additionally, a specific protein kinase A inhibitor, PKI, partially decreased the K^+ currents that were active in the absence of cAMP (Li et al., 1994b), as if an endogenous, constitutively active protein kinase A partially supported their activity. Thus, although it appears that phosphorylation can partially augment the activity of the outward-rectifying plant K channel, it is not known whether its activity can occur in the absence of phosphorylation. Furthermore, all of these studies were conducted either on intact cells, in which the cytosol is largely unperturbed (Armstrong et al., 1995), or on whole protoplasts perfused through a pipette, in which the equilibration of the cytosol with the perfusate might be hampered by the size of the diffusing molecules or by leakage from organelles into the cytosol. Therefore, it is not clear to what extent the proposed phosphorylation requires cytosolic components.

These two questions were addressed in the present work with respect to the outward-rectifying, K_D channel (K_{out}) in protoplasts from the leaf-moving organ (pulvinus) of *Samanea saman* (Satter et al., 1988). This ubiquitous K_D serves as the pathway for K^+ efflux from plant cells. It may play a role in electrical signaling across the plant (Pickard, 1973; Sussman, 1992; Wildon et al., 1992; Stoeckel and Takeda, 1993) and in turgor regulation. Turgor regulation, a widespread phenomenon in most plant cells, is particularly prominent in motor cells such as guard cells and pulvinar cells. A "shrinking" signal (such as darkness) to the *S. saman* extensor cell leads to osmotic volume decrease through the loss of K^+ ions via the K_D channels. This is part of the mechanism of the characteristic nightly leaflet fold-

[1] This research was supported by grants from the Israel Science Foundation administered by the Israel Academy of Sciences and Humanities (ISF, 487/89), the U.S.-Israel Binational Science Foundation, Jerusalem, Israel (BSF, 91–00293), the U.S.-Israel Binational Agricultural Research and Development Fund (BARD, IS-1670–89RC), and the Helen and Milton Kimmelmann Center for Biomolecular Structure at the Weizmann Institute.

* E-mail bnmoran@wicc.weizmann.ac.il; fax 972–8–9344–140.

Abbreviations: AMP-PNP, 5′-adenylylimidodiphosphate; ATPγS, adenosine-5′-O-(3-thiotriphosphate); BAPTA, 1,2-bis(2-aminophenoxy)ethane-*N*,*N*′,*N*′-tetraacetic acid; E_K, calculated equilibrium potential; E_M, membrane potential for K; E_{rev}, reversal potential of the measured current; G_K, conductance for K of the whole-cell membrane; γ_s, unitary conductance; H7, 1-(5-isoquinolinesulphonyl)-2-methylpiperazine; I, whole-cell current; I_K, whole-cell K current; i_s, unitary (single-channel) current; K_D channels, depolarization-activated K channels; $\bar{n}$, average number of open K_D channels.

ing (Satter et al., 1988) and stomatal closing (Hedrich and Schroeder, 1989).

The activity of the K_D channel was monitored with the patch-clamp technique combining whole-cell and single-channel recording. The experiments described here suggest strongly that the K_D channel itself, or an intimately related regulatory protein, undergoes phosphorylation. It is also suggested here for the first time, to our knowledge, that (a) phosphorylation is a prerequisite for the activation of the K_D channel by depolarization, (b) this phosphorylation does not require cytosolic components, and (c) the putative kinase involved is located in the membrane in tight association with the K_D channel. Preliminary results of these studies appeared in an abstract form (Moran, 1993, 1994).

MATERIALS AND METHODS

Samanea saman (Jacq.) Merr. trees were grown in a greenhouse under a schedule of 16 h of light/8 h of dark, as described previously (Moran et al., 1988). Protoplasts were enzymatically isolated from an extensor part of the motor organ (pulvinus) tissue during 3 to 8 h of light. The isolation procedure (Moran et al., 1990) was modified as follows: (a) the osmolarity of the enzyme solution was increased with sorbitol to 780 mosmol, and the osmolarity of the protoplast incubation solution (following enzymatic digestion) was maintained at 720 mosmol; (b) both centrifugations for protoplast purification were at 40*g*; (c) the last step of purification was on a Suc/sorbitol gradient, as described by Moran et al. (1988); and (d) proteinase inhibitor PMSF was included in the digestion medium (0.1 mM from a stock solution in ethanol; final ethanol concentration, 0.1% [v/v]).

Experimental Procedure

The experiments were conducted at room temperatures between 23 and 25°C, but the temperature did not vary by more than 1°C during a single experiment. Application of the patch-clamp methodology (Hamill et al., 1981) to *S. saman* protoplasts was described by Satter and Moran (1988) and Moran et al. (1988). Patch-clamp pipettes were prepared from borosilicate or alumosilicate glass (catalog no. 6160 or 5820, respectively; AM-Systems, Everett, WA) by a two-stage pull and fire polishing, yielding tips with resistance (measured in the recording solutions) between 8 and 15 MΩ for the whole-cell experiments and 20 to 50 MΩ for the single-channel recording. The experiments were performed between 2 PM and 2 AM in a dimly lit room (approximately 1 μmol s^{-1} m^{-2}) under green-filtered microscope illumination (interference filter with 50% of transmission centered at 540 ± 30 nm). The protoplasts were added into a 200-μL chamber, allowed to settle for 5 to 10 min on the glass bottom, and flushed with 10 volumes of the external recording solution at a rate of 1 mL min^{-1}.

For experiments with whole cells (or outside-out patches), the pipette was filled with "internal" solution (see below), and for those with cell-attached and inside-out patches, the pipette was filled with external solution. The bridge of the reference electrode was filled with the alternate solution. After establishing a tight seal with the cell membrane, one of two procedures was adopted. For experiments with whole cells, the membrane was ruptured by gentle suction through the pipette to attain the whole-cell configuration. For experiments with single-channel recording (other than outside-out) the bath was flushed with 10 volumes of internal solution and then recording was performed from a cell-attached patch, or the patch was excised into an inside-out configuration. Outside-out recording was performed with external solution in the bath. Additives were supplied by perfusion in the bath solution. In some experiments ATPγS was applied by diffusion from an adjacent 10- to 15-μm-diameter pipette filled with the internal solution containing 100 μM of the nucleotide. In such cases the nominal ATPγS concentration at the cytoplasmic side of the channel is stated as <100 μM. The bath solution was refreshed by flushing 2 to 3 volumes of the same solution every 10 to 15 min.

All experiments were performed in a voltage-clamp mode using an amplifier (Axopatch B-1; Axon Instruments, Foster City, CA) and were under computer control (a PC 386) using a software-hardware system from Axon Instruments (version 5.5.1, pClamp program package software) and the TL1- TM-100 Labmaster A/D and D/A peripherals). E_M was varied according to preprogramed pulse protocols (detailed below).

The liquid junction potential between the recording solutions was below 1 mV as calculated using ion mobilities and activities (Robinson and Stokes, 1965), and therefore no correction was performed. The error in the voltage clamping of the whole-cell membrane, largely due to the access (series) resistance of the patch pipette (R_s), was compensated at approximately 80% by the analog circuitry of the amplifier. Assuming that in the whole-cell configuration the electrical series resistance reflects the access to ion diffusion (and to other solutes as well) between the cytosol and the interior of the patch pipette, only those experiments with initial R_s ranging between 10 and 25 MΩ, in which the R_s did not vary by more than a few megaohms were included.

The resulting membrane current was filtered at 20 to 100 Hz (the −3-db cutoff frequency of a four-pole Bessel filter) and digitized at a sampling rate of 80 to 200 Hz, respectively. To simplify comparisons between experiments performed in the different configurations in all of the figures, channel openings and outward current (with respect to the membrane) are shown as positive upward deflections from the closed-level (baseline) current. Likewise, in all of the experiments presented here, increasing (i.e. applying more positive) potential at the cytoplasmic side means depolarization. Between depolarizations the membrane was held for 10 to 30 s at a "resting" or "holding" potential of −80 or −100 mV (cytoplasmic side negative), at which K_D channels are closed (Moran et al., 1988).

K channels were activated by depolarization, applied in the form of square pulses (as depicted in the figures) or as ramps varying linearly with time. The protocols using square pulses were used when the currents varied little with time. For the fast determination of G_K and E_{rev}, par-

ticularly during the channel "rundown" experiments, combined quick-ramp and square pulses were used (in whole cells exclusively) as follows: A 170-ms voltage ramp, from +50 to −100 mV or from +70 to −100 mV, was run twice. The first ramp was preceded by a brief (only 20- to 30-ms long) depolarization to +50 or +70 mV, which was too short to allow current activation. This ramp produced a current leak at all E_Ms scanned. Following a 10-s interval at a holding potential of ≤−80 mV, the E_M was stepped to the same depolarizing potential for a longer duration of 6.5 s, which opened the K_D channels. Then, the second ramp (identical with the first) was applied. This ramp produced an activated K^+ current (plus leak current) at all E_Ms scanned. The ramp was very brief relative to the seconds-long deactivation time constant of the *S. saman* K_D channel, as evidenced by the undiminished current recorded when the depolarization was restored immediately after the ramp (data not shown). Therefore, the variation in this current during the ramp did not reflect K_D channel kinetics but only the varying driving force ($E_M - E_{rev}$; see Eq. 1 below).

Slow ramps were used exclusively in single-channel recording for the simultaneous determination of the E_{rev}, γ_s, and the level of channel activity. These were 53-s-long voltage ramps from −100 to +30 mV or from −85 to +45 mV, separated by ≥10-s intervals at −100 mV. The rate of change of the E_M (130 mV/53 s) was slow relative to the few-seconds-long time constant of K_D channel activation (Moran et al., 1988). Therefore, channel activity was assumed to have attained a steady state at each point during the ramp.

In some single-channel experiments, currents were also recorded in steady-state conditions during continuous depolarization to various E_M levels, each lasting several tens of seconds.

Analysis

Determination of G_k and E_{rev} in Whole-Cell Experiments

The separate values of G_K and E_{rev} were determined from the K^+ current-voltage relationship (I_K–E_M) of the depolarized whole cell using Equation 1 (Hodgkin and Huxley, 1952):

$$G_K = I_K/(E_M - E_{rev}). \quad (1)$$

G_K was obtained from the leak-corrected whole-cell instantaneous "tail-current" I_K–E_M relationships as described by Moran et al. (1990) or using the fast ramps, described above, as follows. The two current-voltage (I–E_M) relationships produced by the two voltage ramps, the leak current versus E_M and the activated K^+ current versus E_M, were superimposed. G_K was calculated as the difference between the slopes of these two I–E_Ms. E_{rev} was obtained at their intercept. When compared, the methods for G_K and E_{rev} determination gave similar results.

G_K values chosen for comparisons between treatments were at +50 mV and 15 min after forming the whole-cell configuration, or 10 min after the initiation of the treatment. To minimize variability, the values of G_K from different experiments were first normalized to their individual maximum values (attained at various times in different cells) and only then averaged. Mean G_K values (and their SE values) are therefore presented in relative units.

Determination of γ_s and E_{rev} in Single-Channel Experiments

The γ_s and E_{rev} were estimated from the single-channel current-voltage relationship (i_s–E_M) in a manner similar to that described in Equation 1. i_s–E_M was obtained either directly, by manual linear regression to current responses to ramp commands, or from the amplitude histograms of current recorded at various constant E_Ms (Ilan et al., 1994).

Calculation of $\bar{n}$

The $\bar{n}$ is the product of N, the difficult-to-determine number of channels in the patch (Horn, 1991), and P_o, their open probability (provided, of course, that they are identical and statistically independent [Ehrenstein et al., 1970]). If N remains constant throughout the experiment, variations in $\bar{n}$ reflect the changes in P_o. $\bar{n}$ was calculated from all-points amplitude histograms of the steady-state portion of current records obtained at a constant E_M (Ilan et al., 1994). In the case of square pulses, the current during the second half of the pulse was used. Alternatively, when E_M varied in a ramp, $\bar{n}$ was calculated point by point by subtracting the linearly fitted baseline (leak current) and dividing the record by the linearly fitted i_s amplitude at the same potential.

The resulting steady-state $\bar{n}$–E_M relationships were then fitted with the Boltzmann relationship to obtain the best estimate of $\bar{n}$ at the various E_M values:

$$\bar{n} = \bar{n}_{max}/(1 + e^{-zF(E_M - E_{1/2})/RT}) \quad (2)$$

where $\bar{n}_{max}$ is the maximum mean number of open channels in the patch; $E_{1/2}$ is the half-activation voltage; and z is the effective number of gating charges. $\bar{n}$ values from different treatments were compared at E_M = 0 mV and t = 10 to 15 min after a change in conditions. Wherever required, such values were obtained by interpolation, using the fitted Boltzman relationship or a manually fitted time course of $\bar{n}$. These calculations and fit were performed using a commercially available program (Origin; Microcal Software, Northampton, MA).

Statistics

Differences between means were deemed significant if, using a two-sided t test, P was ≤0.05. The E_{rev} was obtained as the zero-current intercept of a linear regression to current-voltage data points, and its asymmetrical lower and upper 95% confidence limits were calculated by inverse regression (Sokal and Rohlf, 1981).

Recording Solutions

The regular extracellular solution contained 5 mM K^+, 10 mM Mes, pH 6.0, and 0.5 to 1 mM $CaCl_2$ and was adjusted with sorbitol to 780 mOsmol. The extracellular bath solu-

tion for recording from cell-attached patches contained, in addition, 100 mM KCl, with the appropriate adjustment with sorbitol. The cytoplasmic surface was exposed to 125 mM KCl, 20 mM Hepes, adjusted with 8.5 mM *N*-methylglucamine or with 8 mM KOH to pH 7.2 to 7.4, 1 mM K_2ATP, with or without 1 mM $MgCl_2$, 2 mM BAPTA-K_4, and 1 mM $CaCl_2$ (free Ca^{2+}: 100–200 nM, using the dissociation constant of BAPTA with or without 1 mM Mg^{2+}, respectively [Pehtig et al., 1989]). When buffering Mg^{2+} to a very low concentration in the whole-cell internal solution, we used 5 mM EDTA to replace BAPTA, with 4.4 mM $CaCl_2$ and 0.2 mM $MgCl_2$. The free Ca^{2+} concentration was calculated using "Free Calcium," a public domain implementation for Macintosh of a program by Fabiato (1988) and was found to be 160 to 270 nM (at the respective pH of 7.4–7.2); the concentration of Mg^{2+} was 1 μM. For experiments with whole cells, the cytoplasmic solution was adjusted with sorbitol to a final osmolarity of 830 mosmol. For experiments with inside-out patches, both solutions were usually adjusted to a similar osmolarity, 780 mosmol.

The nucleotides and BAPTA were dissolved in 0.5 M *N*-methylglucamine-Hepes buffer (pH 7.2) and kept frozen at −20°C. They were used within 1 week of preparation. All kinase inhibitors were kept frozen at −20°C and diluted as follows during the experiment: H7 · HCl (HCl-derivative in H_2O) and H7 (free base in DMSO): × 400 to 3000; GF109203X (in DMSO): x 1000 to 2500; staurosporin (in DMSO): x500 to 2000. DMSO added at concentrations up to 0.3% (v/v) did not affect channel behavior. H7 · HCl was from Research Biochemicals International (Natick, MA); BAPTA was from Molecular Probes (Eugene, OR), and GF109203X was the kind gift from Dr. H. Coste (Glaxo Institute of Molecular Biology, Geneva, Switzerland). Other chemicals were from Merck or Sigma.

RESULTS

ATP and Mg^{2+} Prevent Channel Rundown

When the K_D channels in the plasma membrane of *Samanea* extensor cell protoplasts were activated repeatedly by depolarization in the absence of MgATP in the internal solution, the whole-cell current through these channels diminished gradually (Fig. 1, A and B). Similarly, the whole-cell conductance declined rapidly in five of five cells (Fig. 1C, squares). In contrast, when the patch pipette contained 1 mM MgATP, the conductance did not decline for 30 min after establishing the whole-cell configuration (Fig. 1C, circles, n = 21). The average maximum values of the specific conductance (i.e. normalized to cell surface) were not significantly different with or without MgATP (0.58 ± 0.06 and 0.82 ± 0.18 mS cm^{-2}, respectively [±SE]). However, the two time courses of conductance differed significantly (one-factor analysis of variance, $P < 0.05$).

It is interesting that in whole cells omission of Mg^{2+} from the ATP-containing internal solution prevented the decay of conductance, which remained comparable to that of the control solution (Fig. 1C, triangles). However, when the internal Mg^{2+} concentration was buffered with EDTA to approximately 1 μM (see "Materials and Methods"), the whole-cell conductance declined to 25% within 20 min after breaking into the cell (n = 2; not shown). This suggests that the unbuffered solution may have contained Mg^{2+} that leaked into the cytosol from internal compartments such as vacuoles or chloroplasts.

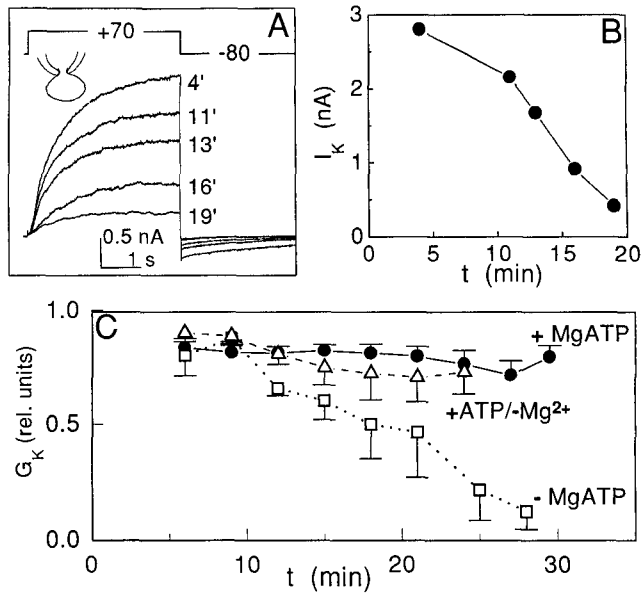

Figure 1. MgATP is required to maintain the activation of K_D channels by depolarization. A, Whole-cell outward currents (superimposed) elicited by a repeatedly applied pulse from −80 to +70 mV (top, E_Ms indicated in mV) in a whole-cell configuration (inset). Numbers at the right of the current traces indicate the time (in min) after creating the contact between the pipette interior and the cytoplasm. The internal solution did not contain MgATP. The filter cutoff frequency was 20 Hz. B, The steady-state, leak-corrected, I_K versus the time elapsed from breaking into the cell. C, The time course of the steady-state conductance, G_K (means ± SE, relative units), at a depolarization to 70 mV, with 1 mM MgATP (●, n = 21), 1 mM ATP and 0 added Mg^{2+} (△, n = 9), or 0 added MgATP (□, n = 5) in the pipette. The comparison of rundown rates of conductance in whole-cell experiments involved (a) approximating by linear regressions the individual time courses of conductance of each cell, starting at min 6 after breaking open into the cell, (b) using one-factor analysis of variance of slopes of these regressions grouped by treatment (using StatView, version II, a commercially available Macintosh application), followed by Scheffe's multicomparison procedure (at α = 0.05; Winer, 1971).

To avoid the interference between the cell contents and the experimental solutions, and thus to resolve the direct effects of the latter on the conducting pathways, experiments were also performed on excised membrane patches. This required determining the identity of the single channels in the patches based on their voltage and time dependence and on their conductance and ion selectivity. The identification of the K_D channels is illustrated most convincingly in the comparison of the macroscopic whole-cell currents and unitary K_D channel currents recorded from an outside-out patch excised immediately following the recording from a whole cell (Fig. 2).

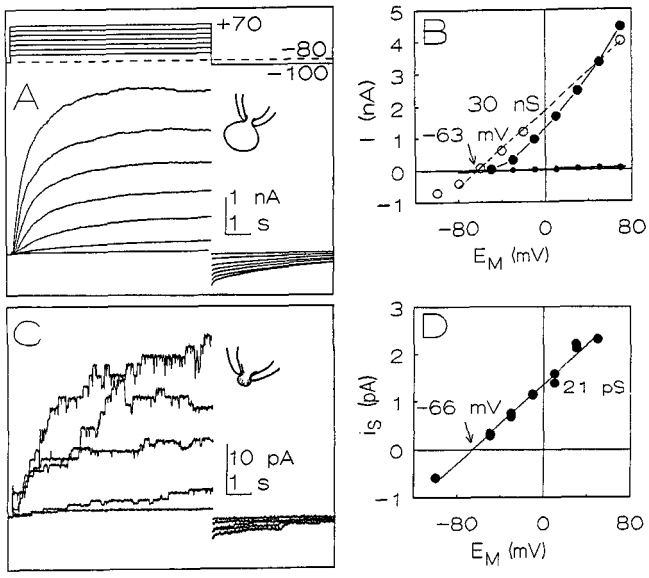

Figure 2. K_D channels in a patch represent channels in the whole cell. A, Whole-cell outward currents (traces superimposed at the bottom) elicited by a series of depolarizing square voltage pulses increasing in steps of 20 mV from −50 to +70 mV (top; see "Materials and Methods"; numbers indicate E_Ms in mV). Inset, The recording configuration. The filter cutoff frequency was 20 Hz. B, Current-voltage (I–E_M) relationships of the cell as shown in A. Small circles, "Leak" I–E_M at the start of the pulses; large circles, steady-state I–E_M at the end of the pulses; and "tail," the instantaneous I–E_M (see "Materials and Methods") at the instant after a jump from +70 mV to several potentials, indicated on the abscissa (o). The solid lines were fitted to the data by eye. The dashed line indicates the linear regression to the instantaneous tail I–E_M. The slope of – – –O– – – (the whole-cell conductance at the end of the +70 mV depolarization) was 30 ± 1 nS (±SE) and the E_{rev} (indicated by arrow) was −63 mV (with 95% upper and lower confidence limits of −75 and −52 mV, respectively, see "Materials and Methods"). C, Single-channel outward currents (the traces are superimposed) from an outside-out patch (inset) excised from the same cell as in A, elicited by the five highermost pulses of those shown in A. Filter was 20 Hz. D, Single-channel current-voltage (i_s–E_M) relationship. Symbols are the amplitudes of the i_s jumps. Line is the linear regression to the data; slope (γ_s) was 21 ± 1 pS (±SE), and the E_{rev} (arrow) was −66 mV (with 95% confidence limits of −80 and −53 mV). Note the 1000-fold difference in the current scales between B and D.

Voltage and Time Dependence

Increasingly larger depolarizing voltage pulses elicited progressively larger currents in the whole-cell membrane (Fig. 2A). Their voltage dependence at steady state is summarized in Figure 2B (large, solid circles). The time dependence of the whole-cell currents matched the gradual recruitment of single open channels in the patch, seen as "staircases" of current jumps in Figure 2C. The larger the pulse, the more channels were activated simultaneously; up to 16 channels were open simultaneously at the end of the largest pulse (Fig. 2C).

Open-Channel Conductance

Neither the instantaneous nor the single-channel current rectified with voltage (Fig. 2B, dashed line, and Fig. 2D, line), justifying the use of Equation 1 (see "Materials and Methods"). The γ_s in this patch was 21 pS (Fig. 2D). The linear current-voltage relationship also characterized the K_D channels in inside-out patches; their conductance was 19 ± 2 pS (mean ± SD, n = 13).

Selectivity

The E_{rev}s of the I_K and the i_ss in this experiment were nearly identical (−63 and −66 mV, respectively; Fig. 2, B and D). The E_{rev} of i_s (determined in inside-out patches) was −74 ± 1.4 mV (mean ± SE; n = 13). Thus, the E_{rev} values of Figure 2 were well within the distribution of the E_{rev} values determined in other single-channel experiments. The whole-cell E_{rev} deviated from E_K by 7 ± 1.3 mV (mean ± SE, n = 18). In both the whole cells and single channels, the deviations from the calculated K^+ equilibrium potential (E_K of −79 or −80 mV, depending on the internal solution; see "Materials and Methods") were significant (two-sided t test, $P < 0.01$). Since the equilibrium potentials of the other potentially permeant ions in the recording solutions (Cl^-, Ca^{2+}, and H^+) were positive (100; >110, and >70 mV, respectively), the deviation of the single-channel E_{rev} from E_K can be explained by the small permeability to any of these ions. For example, assuming the K_D channel to be permeable to Ca^{2+} (Inoue, 1981; Fairley-Grenot and Assmann, 1992; Manor and Moran, 1994), with 0.25 of the permeability to K^+, and using the Lewis modification of the Goldmann-Hodgkin-Katz potential equation (Lewis, 1979) would yield the mean value of the single-channel E_{rev} obtained experimentally, −74 mV. It should be noted that, even with this apparently large assumed relative permeability to Ca^{2+} in the K_D channel, the ratio between the inward Ca^{2+} current and the outward K^+ current, calculated using the Goldmann-Hodgkin Katz current equation (reviewed by Hille, 1992) will remain below 1% at all potentials more depolarized than −10 mV. If, additionally, the whole-cell membrane is permeable to Cl^- (with only 0.005 of the permeability to K^+), the calculated E_{rev} of the whole cell will equal the mean experimental value of −72 mV. Thus, the whole-cell conductance is satisfactorily represented by the single K_D channels in isolated patches.

In the following experiments K_D channels were identified in isolated patches by their activation by depolarization and by their current-voltage relations.

To examine whether Mg^{2+} is required for K_D channel activity, inside-out patches were excised into cytoplasmic solution containing 1 mM ATP without Mg^{2+} (n = 4). The channels were identified by their current-voltage relation at an intermediate stage of rundown (Fig. 3B). The almost immediate loss of K_D channel activity was striking; in no case was channel activity observed more than 5 min after patch excision. Figure 3A illustrates such a transition: A depolarizing pulse activated at least seven K_D channels in a cell-attached configuration, whereas 1 min after excision, in the same patch of membrane, only one channel opening was observed. In contrast, in control experiments with inside-out patches facing internal solutions containing 1

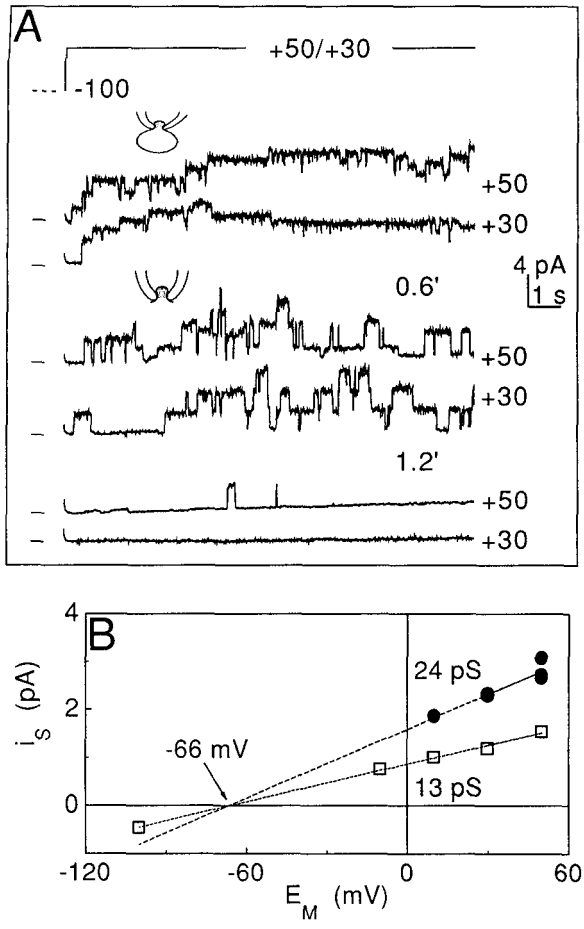

Figure 3. Mg^{2+} is essential for maintaining K_D channels' responsivity to depolarization. A, Single-channel currents during step depolarizing pulses (top) to +30 and +50 mV (indicated in mV at the right of the current traces), in one membrane patch, first in a cell-attached, then in an inside-out configuration (insets). Holding potential was −100 mV. Dashes at the left indicate current levels with all channels closed. Note the characteristic recruitment by depolarization of open channels in the cell-attached mode and the loss of activity at the indicated times (minutes) after patch excision from the cell into a Mg^{2+}-lacking solution (with 1 mM $ATPK_2$). Filter was 20 Hz. B, Identification of the K_D channel. Single-channel current-voltage relationships (i_s–E_M) in a cell-attached (□) and inside-out configurations (●). Only the larger channel is considered here. Lines show linear regressions to the data points. The γ_s changed from 13.1 ± 0.4 to 24 ± 4 pS (±SE) upon excision. The E_{rev}s were −66 mV, both before and after excision (with 95% upper and lower confidence limits of −53 and −79 mV and −29 and −171 mV, respectively). The γ_s increase is most likely due to the increase in the K^+ concentration at the cytoplasmic side of the membrane, from an unknown value in the intact cytosol to 143 mM in the internal experimental solution in the bath. The identity of the E_{rev} before and after excision, when the intracellular K^+ concentration is different from that of the bath, can be accidental, resulting from a particular combination of the E_{rev} of the membrane of the whole cell with the additional hyperpolarizing action of the plasma membrane proton pump. Alternatively, if the K_D channels in the patch and the membrane of the whole cell behave like a K^+ electrode, the E_{rev} should depend on the ratio of concentrations of K^+ in the pipette and the bath even in the cell-attached configuration, irrespective of the internal K^+ concentration (Manor and Moran, 1994).

mM MgATP, 15 min after patch excision, $\bar{n}$ was 5.9 ± 1.8 (±SE, n = 7; Fig. 4C).

ATP was also necessary to preserve K_D channel activity. In inside-out patches excised into ATP-free solution (containing 1 mM Mg^{2+}) this activity diminished usually within several minutes (Fig. 4, A and B). At 15 min and 0 mV, the

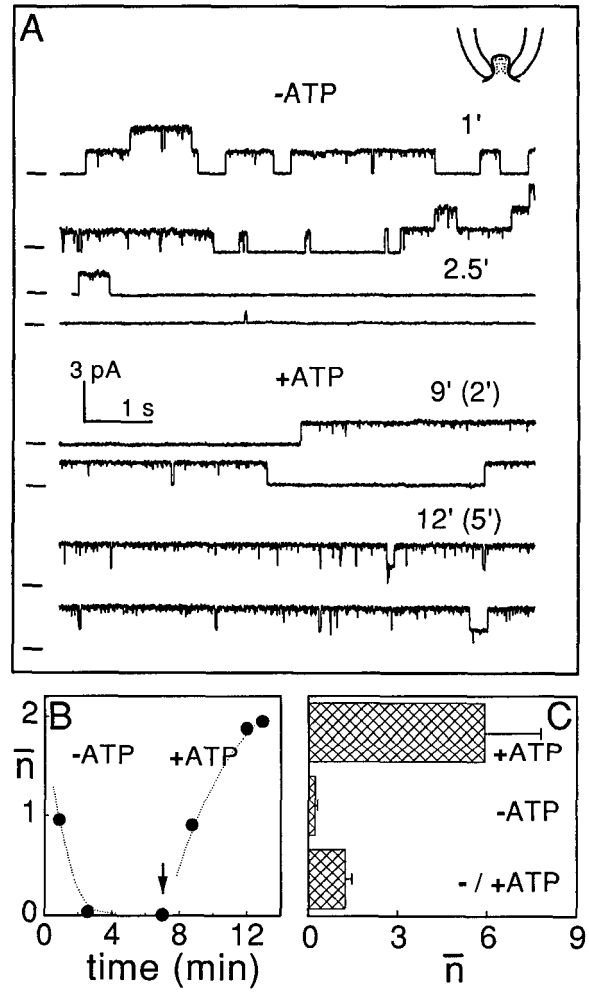

Figure 4. ATP can restore rundown channels. A, i_s fluctuations (sample records) during continuous depolarization to −10 mV (cytoplasmic side negative), at an inside-out configuration (inset), at the indicated times (minutes) after patch excision into ATP-free cytoplasmic solution (containing 1 mM Mg^{2+}). Numbers in parentheses indicate time since the start of solution change to one containing 1 mM ATP. Dashes at the left indicate current levels with all channels closed. Single-channel conductance, γ_s, in the presence of ATP, was 21 ± 0.4 pS (±SE), E_{rev} was −87 mV with 95% upper and lower confidence limits of −72 and −102 mV, respectively. Filter was 100 Hz. B, $\bar{n}$ indicates the mean number of open channels (calculated as described in "Materials and Methods") versus time after patch excision, in records lasting 33, 15, 20, 59, 58, and 45 s, respectively (data are plotted versus the midpoints of the record periods). The arrow indicates the introduction of ATP. Line was fitted by eye to the data points. C, $\bar{n}$ at 0 mV and at 15 min after inside-out patch exposure to a solution (from top to bottom) containing MgATP (5.9 ± 1.8, n = 7), lacking ATP (0.2 ± 0.09, n = 7), and at 3 to 10 min after reapplication of ATP (1.2 ± 0.2, n = 5). The differences among all of these means were significant.

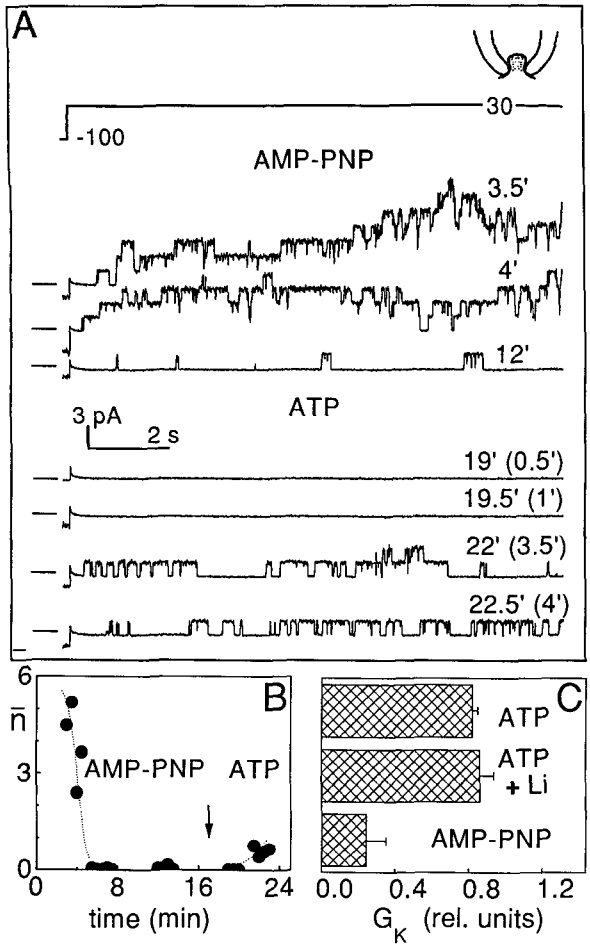

Figure 5. AMP-PNP does not sustain K_D channel activity. A, Sample records of currents elicited in an inside-out patch (inset) by repeated depolarizing pulses from −100 to +30 mV (top trace). Interpulse interval was 21 s. Numbers (minutes) indicate the times (at mid-record points) after patch excision into internal solution containing 1 mM of the nonhydrolyzable analog of ATP, AMP-PNP. Note the recruitment of open channels upon depolarization at 3 to 4 min, the rarity of openings at 12 min, and the renewal of channel activity 3 to 4 min after replacing AMP-PNP with 1 mM ATP. Numbers in parentheses indicate the time since the nucleotide substitution. γ_s, in the presence of ATP, was 25 ± 4 pS (±SE), E_{rev} was −63 mV with 95% upper and lower confidence limits of −28 and −119 mV, respectively. Filter was 50 Hz. B, The time course of $\bar{n}$ in the patch of A. The arrow indicates the change of solutions. C, G_K (in relative units) at 15 min after exposure of the cytoplasmic side to internal solution containing (top to bottom) 1 mM ATP (0.82 ± 0.03 [mean ± SE]; n = 21), 4 mM Li^+ added to 1 mM ATP (0.86 ± 0.08; n = 3), and 1 mM AMP-PNP as the sole nucleotide (0.24 ± 0.11; n = 6). The differences between the two controls and the AMP-PNP treatment were significant.

$\bar{n}$ was 0.2 ± 0.09 (±SE, n = 7; Fig. 4C). The rundown of channel activity was reversible: ATP reapplied to the cytoplasmic side of the membrane (in the presence of Mg^{2+}) after no channel openings could be evoked by depolarization, restored channel activity. In five of five such attempts, $\bar{n}$ increased to 1.22 ± 0.22 within 3 to 10 min after reapplication of ATP (Fig. 4C).

ATP Analogs

To test whether hydrolysis of ATP is required for retaining K_D channel activity, inside-out patches were exposed to bath solutions containing Mg^{2+} (1 mM) and a nonhydrolyzable analog of ATP, AMP-PNP (1 mM). In the presence of AMP-PNP, channel activity declined from at least seven channels open simultaneously 3.5 min after excision to

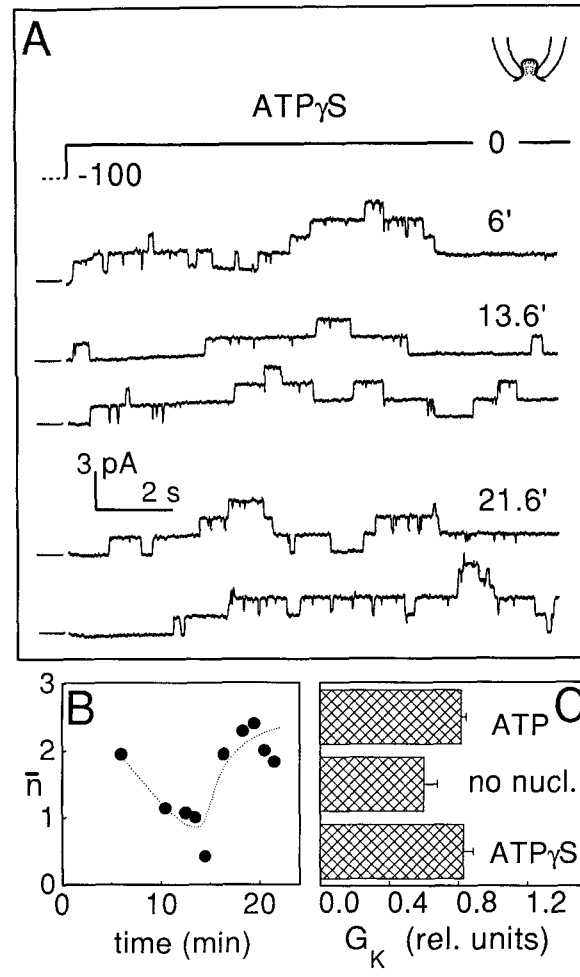

Figure 6. ATPγS mimics ATP in restoring channel activity. Sample records of unitary K_D channel currents elicited by repeated depolarizing pulses from −100 to 0 mV (A) in an inside-out patch (inset) excised into an ATP-free cytoplasmic solution containing 1 mM Mg^{2+} and 30 μM ATPγS. The dashes at the left indicate current level when all channels are closed. Numbers indicate mid-record times (in minutes) after patch excision. γ_s was 16 ± 1 pS (±SE), E_{rev} was −82 with 95% upper and lower confidence limits of −71 and −95 mV, respectively. B, The time course of $\bar{n}$ of the patch in A, calculated from the second halves of the individual records (see "Materials and Methods"). Note the initial decline and the subsequent increase of $\bar{n}$. Filter was 20 Hz. C, G_K in whole cells (in relative units), at 15 min after exposure of the cytoplasmic side to the internal solution containing (top to bottom) 1 mM ATP (0.82 ± 0.03 [mean ± SE]; n = 21), no nucleotides (0.6 ± 0.08; n = 5), and 50 μM ATPγS as the sole nucleotide (0.83 ± 0.06; n = 5). Only the difference between the mean of the treatment with ATP and that without nucleotides was significant.

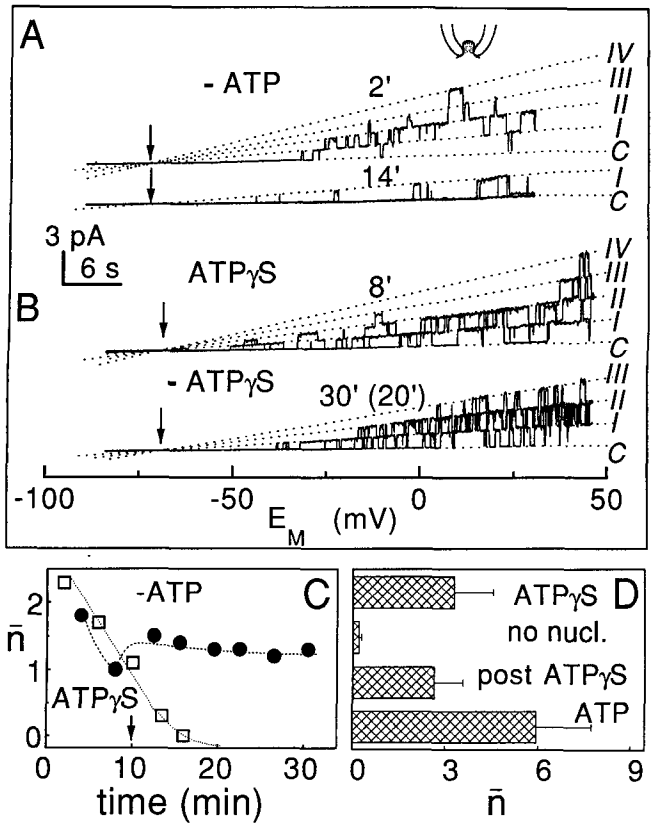

Figure 7. ATPγS effect is irreversible. A and B, Single-channel currents evoked in two inside-out patches (inset) from the same cell, by slow voltage ramps. Abscissa shows the values of E_M during the ramps. Because voltage changed linearly with time during the ramp (130 mV/53 s), the currents can be viewed simultaneously as a function of time (horizontal scale bar) and as a function of E_M (abscissa). Dotted lines indicating the expected linear i_s–E_M relationships of 0, 1, or 2, etc., simultaneously open channels, were fitted by eye to the closed level (indicated by *C* at the right) and to the various open current levels (indicated at the right by roman numerals). Numbers indicate the time (in minutes) elapsed since patch excision to the midpoints of the recording periods. Filter was 20 Hz. A, K_D channel rundown in the absence of ATP in the cytosolic solution. A single-current response during a single ramp is shown at the top, and three superimposed responses to three consecutive ramps (during a total of 4 min) are shown at the bottom. The γ_s (the average increment in the slope between the neighboring fitted linear i_s–E_Ms) was 20 pS. The current E_{rev} (marked by an arrow) was −72 mV. B, Inhibition of rundown by transient exposure to ATPγS. Currents are as in A. During the first 10 min after patch excision into solution without ATP, the cytoplasmic side of the patch was exposed to ATPγS diffusing from an approximately 10-μm orifice of a pipette positioned approximately 15 μm away, containing 100 μM ATPγS. The ATPγS pipette was then lifted out of solution (arrow), and the patch pipette was moved to the other side of the chamber, approximately 5 mm away. Numbers in parentheses denote the time since the termination of the exposure to ATPγS. γ_s was 18 pS; E_{rev} was −69 mV. C, The time course of at E_M = 0 mV (see "Materials and Methods"). Squares indicate $\bar{n}$ in the patch of A; circles indicate $\bar{n}$ in the patch of B; lines were fitted by eye to the data points. Note the transient decline of channel activity in the presence of ATPγS and the persistence of channel activity after nucleotide removal (circles). D, Mean $\bar{n}$ in inside-out patches at E_M = 0 mV and at 15 min after exposing the cytoplasmic patch surface to internal solution containing (from top to bottom) 25 to <100 μM ATPγS (3.28 ± 1.26; n = 10); no nucleotides at all (0.2 ± 0.09; n = 7); no nucleotides after a transient exposure (for 10–15 min) to 25 to <100 μM ATPγS (2.63 ± 0.94; n = 3); and 1 mM ATP (5.9 ± 1.8; n = 7). The mean $\bar{n}$ values resulting from both the transient and the prolonged treatment with ATPγS were not significantly different from one another or from the control in ATP. All of the treatments differed significantly from the no-nucleotide treatment.

barely one 12 min after excision (Fig. 5, A and B). In four inside-out patches, the activity of the K_D channel subsided completely (to $\bar{n}$ = 0) within 4 to 15 min. A similar decay of activity was also observed in six of six whole cells: their conductance reached the value of 0.24 ± 0.11 (mean ± SE, in relative units) 15 min after attaining the whole-cell configuration (Fig. 5C). In the experiment of Figure 5A, the addition of ATP partially restored channel activity within 3 min (with $\bar{n}$ = 0.6 ± 0.08, mean ± SE of four determinations), demonstrating that AMP-PNP did not have irreversible effects (Fig. 5, A and B). Li^+ alone (4 mM added to 1 mM ATP in whole cells as a control for the Li^+-containing AMP-PNP compound) did not have any inhibitory effect; in its presence the normalized whole-cell conductance was 0.86 ± 0.08; n = 3), which is comparable to the value of 0.82 ± 0.03 (n = 21) in control experiments with MgATP (Fig. 5C).

If phosphorylation is the mechanism by which ATP promotes channel activity, then a hydrolyzable ATP analog should sustain K_D channel activity. To test this, ATP was replaced with ATPγS, which can substitute for ATP in most kinase reactions but is resistant to hydrolysis by phosphatases (Gratecos and Fisher, 1974; Eckstein, 1985). Indeed, in the presence of ATPγS (30 μM) at the cytoplasmic side of the patch, K_D channel activity lasted for more than 20 min after patch excision and a transient decline (Fig. 6, A and B). Fifteen minutes after the whole-cell configuration was attained with only 50 μM ATPγS in the internal solution as the sole nucleotide, G_K in whole cells was indistinguishable from that in control cells faced with 1 mM ATP (0.83 ± 0.06, n = 5, versus 0.82 ± 0.06, n = 21; Fig. 6C). At 15 min, however, any possible difference between G_K in ATPγS treatment and G_K in the no-nucleotide treatment (0.6 ± 0.08, n = 5; compare also with Fig. 1C, squares) was obscured by their variation (although both differed significantly from the ATP control; Fig. 6C). The differences among treatments were much more pronounced in excised patches. In 10 inside-out patches, exposed upon excision to ATPγS (25 to <100 μM) at their cytoplasmic side, $\bar{n}$ at 15 min after excision was 3.28 ± 1.26 (Fig. 7D), which was significantly more than in patches without nucleotides (0.2 ± 0.09; n = 7; Fig. 7D).

If a kinase action is rendered irreversible, K_D channel activity might be expected to persist without nucleotides. To test this, an inside-out patch was presented for 10 min with ATPγS (diffusing from a nearby pipette containing 100 μM ATPγS, which was then lifted out of the bath), and channel activity was examined using slow voltage ramps. Figure 7, A and B, shows K_D channel openings elicited in this and in another inside-out patch from the same cell, without nucleotides. Whereas in the patch without nucle-

otides the activity declined almost completely in 16 min (Fig. 7, A and C, squares), in the patch presented transiently with ATPγS the K_D channel activity persisted for an additional 20 min without significant decay (Fig. 7, B and C, circles; in two patches excised subsequently into the same solution, channel activity diminished fast, indicating the absence of any significant remnants of the nucleotide in the bath). In three of three inside-out patches, 15 min after prior exposure to ATPγS followed by nucleotide removal, $\bar{n}$ was 2.63 ± 0.94 (Fig. 7D). This value was significantly different from that reached during 15 min of rundown in the absence of any nucleotide (0.2 ± 0.09; Fig. 7D).

Inhibition by H7

If kinase action were needed before depolarization could activate the K_D channel, then kinase inhibitor would be expected to inhibit channel activity. To test this, channel activity was examined using kinase inhibitors. H7 is a broad-range kinase inhibitor (Hidaka et al., 1984). At the highest concentration used in this study (100 μM), it was previously shown to block phosphorylation in plant cells (Raz and Fluhr, 1993). H7 is membrane permeant and is presumed to reach its site of action—the kinase associated with channel activity, which presumably resides at the cytoplasmic surface of the membrane—either by diffusing laterally in the membrane or via diffusion through the membrane and into the cytosol. Ten minutes after the bath was flushed with a solution containing 100 μM H7, the fluctuations of the i_ss during 20-mV depolarizing pulses diminished considerably (Fig. 8, A and B), and 5 min later almost none were seen. The time course of the inhibition of channel activity by H7 is illustrated in Figure 8B, which displays $\bar{n}$ in this patch.

H7 inhibited K_D channel activity both in cell-attached patches and in whole cells (Fig. 8C). Ten minutes after the application of an H7-containing bath solution (50–100 μM), the inhibition of channel activity (relative decrease of $\bar{n}$ or of G_K) in cell-attached patches reached 81 ± 5% (n = 3), and in whole cells it reached 75 ± 9% (n = 4). In whole cells treated for 10 min with 14 to 40 μM H7, inhibition reached only 41 ± 9% (n = 3). Channel activity did not diminish within a comparable time in cell-attached patches when H7 was omitted from the bath perfusate (3 ± 12%; n = 3). In whole cells, washing the H7 out reversed the inhibition within 10 min, at least partially, in four of six attempts (Fig. 9). The current was restored, on average, to 73 ± 10% of control (Fig. 9B), showing that its decrease after H7 application was not due to cell deterioration.

Two membrane-permeant protein kinase C-specific inhibitors, staurosporin (0.5–2 μM; n = 6) and GF109203X (20–50 μM; n = 5), applied externally in a whole-cell configuration, were without effect (data not shown).

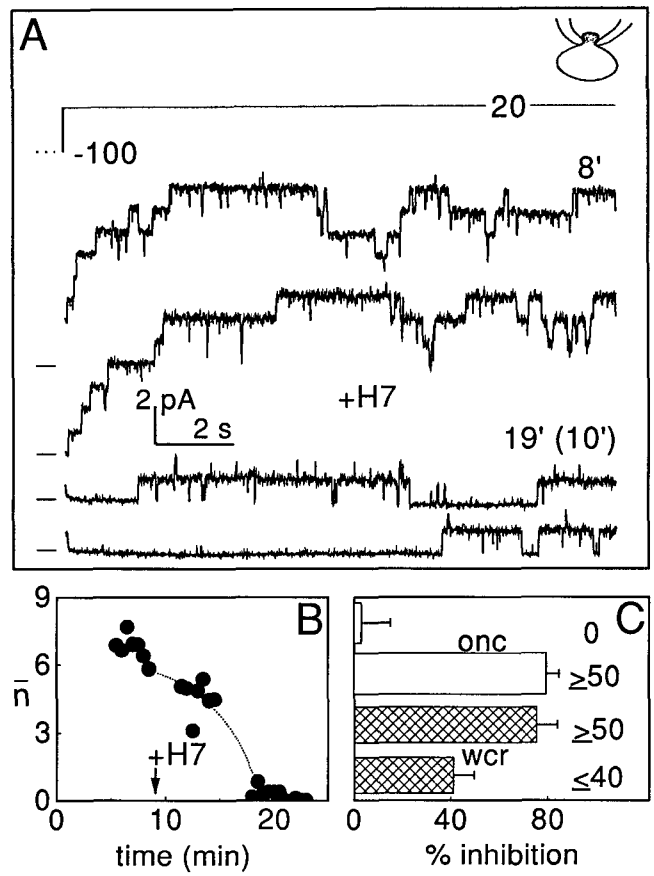

Figure 8. H7 decreases channel activity. A, Sample traces of single-channel currents elicited in a cell-attached patch (inset), by depolarizing pulses from −100 to +20 mV (top trace). Number in parentheses indicates a mid-record time point, measured since H7 addition (100 μM). During the control run, the γ_s was 16 ± 1 pS (±SE), E_{rev} was −61 with 95% upper and lower confidence limits of −49 and −75 mV, respectively (these values of the patch E_M are superimposed on the unknown E_M of the cell). Filter was 100 Hz. B, Time course of $\bar{n}$ in the patch of A. The arrow indicates the administration of H7-containing solution. Note the decline in channel activity. C, Percentage inhibition (i.e. the decrease of G_K or $\bar{n}$ relative to their control values prior to treatment; mean ± SE of n cells) at 10 min after administration of H7. Numbers indicate H7 concentration ranges: ≥50, 50 to 100 μM; ≤40, 14 to 40 μM. onc (white bars) and wcr (hatched bars) signify cell-attached and whole-cell recording configurations, respectively. 0 indicates a flush without H7, applied in control onc recording at a comparable time range (6–23 min; n = 3). Note the relative lack of inhibition within 10 min after the control flush. Note also the similar effectiveness of ≥50 μM H7 in inhibiting channel activity in the cell-attached and whole-cell configurations (79 ± 5%, n = 3 and 75 ± 9%, n = 4, respectively). This inhibition was significantly more pronounced than with ≤40 μM of H7 (41 ± 9%, n = 3).

DISCUSSION

The most prominent effect of the phosphorylating agents described here, ATP and ATPγS accompanied by Mg^{2+}, was the sustainment of K_D channel activity. Application of ATP to the cytoplasmic surface of excised plasma membrane patches also promoted the activity of two types of K channels and a nonselective cationic channel in an Arabidopsis mesophyll cell (Spalding and Goldsmith, 1993) and in an inward-rectifying K channel of *V. faba* guard cell (Wu and Assmann, 1995). The authors did not resolve experimentally the mode of action of ATP (binding versus phosphorylation).

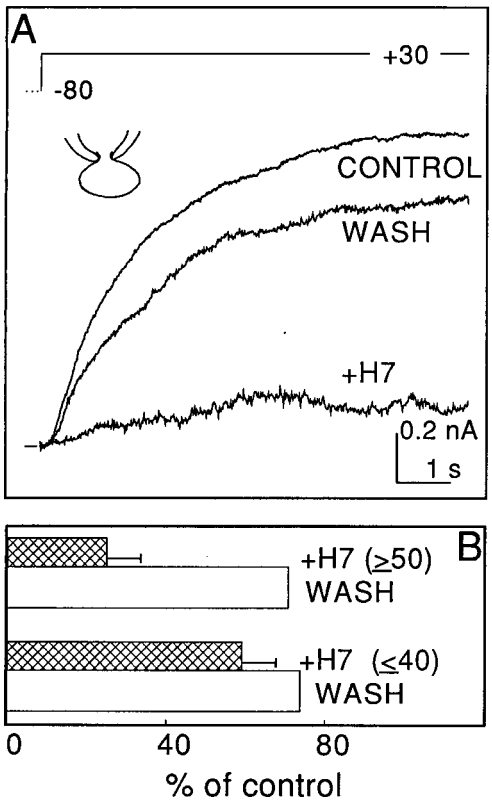

Figure 9. H7 inhibition is reversible. A, Superimposed traces of K_D channel current elicited in a whole cell by step-pulses from −80 to +30 mV, before (CONTROL), during (+H7), and after (WASH) the exposure to 100 μM of H7 in the bath solution. The dash at the left of the traces indicates the current level at the start of the depolarization, prior to K_D channel activation. Leak current has been subtracted. Its values were 28, 164, and 109 pA, respectively. B, Restoration of I_s 10 min after wash, following brief (10 min) treatment with H7. Hatched bars represent whole-cell data (rearranged) of Figure 8C; open bars represent the degree of restoration of channel activity, relative to pretreatment value, in four cells, two at each of the indicated concentration (μM) ranges. The mean increase of current in four cells upon wash was 49 ± 11%.

Modification by Phosphorylation, Not Binding

ATP may have affected the activity of the K_D channel by acting as a ligand, binding reversibly to an allosteric site, similar to the ATP-sensitive K channel in the pancreas or heart (Noma, 1983; Cook and Hales, 1984), or to the cardiac L-type Ca channel, where ATP suggestedly forms an obligatory Mg^{2+}-nucleotide complex (O'Rourke et al., 1992). However, in all of these cases, the nonhydrolyzable analog AMP-PNP successfully substituted for ATP, indicating no need for nucleotide hydrolysis. In contrast, in the experiments presented here AMP-PNP at the same concentrations as used elsewhere did not support K_D channel activity (Fig. 5), indicating that the hydrolysis of ATP was essential for its effect on the K_D channel. The requirement for a simultaneous presence of Mg^{2+} (Figs. 1 and 3) and the hydrolysis of ATP is thus consistent with the requirement for a kinase action.

ATPγS has been widely used as a substrate for kinase activity (Gratecos and Fisher, 1974), particularly in studies involving ion channels (Chung et al., 1991; reviewed by Levitan, 1994). In plants, ATPγS (at 500 μM) almost doubled the outward whole-cell currents through the *V. faba* mesophyll K channels (Li et al., 1994b), although, curiously, it had no apparent effect on their counterparts in the guard cells (Fairley-Grenot and Assmann, 1991). In the present study, the prevention or reversal of rundown of K_D channel activity by ATPγS (in the range of 25 to <100 μM, Figs. 6 and 7, A and B) resembles the effect seen in the mesophyll cells of *V. faba*. Furthermore, the initial transient rundown in the presence of ATPγS (Figs. 6B and 7C), absent in experiments with ATP, is consistent with the reportedly slow thiophosphorylation (Chung et al., 1991). The persistence of the *S. saman* K_D channel activity after subsequent removal of ATPγS (Fig. 7, B–D) is consistent with covalent modification of a protein or proteins in the patch rather than with temporary binding effects of ATPγS.

Finally, the effect of H7 is also consistent with the requirement for phosphorylation. Since the properties of the K_D channel in excised patches seem to represent those in the whole cell (Fig. 2), and the K_D channels in cell-attached patches resemble closely those in excised patches (Fig. 3), it is very likely that in all of these cases K_D channel activity depends on the same putative kinase. Most likely, therefore, it is this K_D channel-related kinase that is the target for the inhibitory H7 effect in whole cells and in cell-attached patches.

The Kinase Identity

Taken together, all of these results strongly support the notion that the K_D channel will not function in the absence of phosphorylation, even though both the kinase responsible for this and the site that undergoes phosphorylation have yet to be identified. Nonetheless, based on the lack of effect of the kinase inhibitors staurosporin and GF109203X, it is possible to eliminate the "classical" protein kinase C or the plant calcium-dependent protein kinase, also blockable by staurosporin (Abo-el-Saad and Wu, 1995). It is also unlikely that a classical cyclic nucleotide-dependent kinase would be activated in the conditions of a whole-cell configuration, particularly in excised patches without an extraneous supply of the cyclic nucleotides. On the other hand, the possibility that the kinase in question is a constitutively active protein kinase A-like protein kinase (as in Li et al., 1994b) needs to be examined.

Structural Considerations

The stimulated increase in the *S. saman* K_D channel activity was observed in excised patches and survived changes of bath solutions. Therefore, the activating regulatory site and its kinase appear to reside in an intimate association with the K_D channel. This is the first such indication for a plant channel. Such tight association of these elements has been already observed in a calcium-activated K channel from rat brain reconstituted in an artificial bilayer (Chung et al., 1991) or in a heterogenously expressed Ca-activated K channel from *Drosophila* in excised patches from *Xenopus* oocytes (Esguerra et al., 1994).

When a clone of the outward-rectifying plant channel becomes available—aided, perhaps, by the recent cloning of the yeast TOK1 channel (Ketchum et al., 1995)—and the channel protein is isolated (Ivanina et al., 1994), it may be possible to resolve whether the phosphorylation site and perhaps even the kinase are part of the neighboring regulatory proteins or part of the channel molecule itself.

Physiological Significance

The opening of the K_D channels (the physiological consequence of the shrinking signals) has been postulated to occur by depolarization (Moran et al., 1988; Hedrich and Schroeder, 1989; Schroeder et al., 1994; Ward et al., 1995). The responsivity to depolarization of the K_D channels in *S. saman* might be governed rhythmically by the circadian "biological clock" (Kim et al., 1993). Phosphorylation, which perhaps mediates the influence of the clock, emerges now as a possible "enabling" regulator of this ubiquitous plant channel, determining whether it will open upon depolarization.

ACKNOWLEDGMENTS

This is another work inspired by the leadership of my late friend and mentor, Ruth Satter. I am grateful to Dr. M. Segal for continuous support and encouragement. Thanks are due to Ms. M. Barzilai, Ms. E. Ziskin, and Ms. L. Katzovay for technical help; to Ms. E. Burg and Ms. N. Barak for help with data reduction; to Drs. G. Ehrenstein, K. Iwasa, M. Bundmann, Y. Shai, and B. Attalie for comments concerning an earlier version of the manuscript; and to Dr. A. Moran for many helpul discussions and suggestions.

Received January 18, 1996; accepted May 10, 1996.

LITERATURE CITED

Abo-el-Saad M, Wu R (1995) A rice membrane calcium-dependent protein kinase is induced by gibberellin. Plant Physiol **108:** 787–793

Armstrong F, Leung J, Grabov A, Brearley, Giraudat J, Blatt MR (1995) Sensitivity to abscisic acid of guard-cell K^+ channels is suppressed by *abil-1*, a mutant *Arabidopsis* gene encoding a putative protein phosphatase. Proc Natl Acad Sci USA **92:** 9520–9524

Chung SK, Reinhart PH, Martin BL, Brautigan D, Levitan IB (1991) Protein kinase activity closely associated with a reconstituted calcium-activated potassium channel. Science **253:** 560–562

Cohen P (1992) Signal integration at the level of protein kinases, protein phosphatases and their substrates. Trends Biochem Sci **17:** 408–413

Cook DL, Hales CN (1984) Intracellular ATP directly blocks K^+ channels in pancreatic B-cells. Nature **311:** 271–273

Eckstein F (1985) Nucleoside phosphorothioate. Annu Rev Biochem **54:** 367–401

Ehrenstein G, Lecar H, Nossal R (1970) The nature of the negative resistance in bimolecular lipid membranes containing excitability-inducing material. J Gen Physiol **55:** 119–133

Esguerra M, Wang J, Foster CD, Adelman JP, North RA, Levitan IB (1994) Cloned Ca^{2+}-dependent K^+ channel modulated by a functionally associated protein kinase. Nature **369:** 563–565

Fabiato A (1988) Computer programs for calculating total from specified free or free from specified total ionic concentrations in aqueous solutions containing multiple metals and ligands. Methods Enzymol **157:** 378–417

Fairley-Grenot KA, Assmann SM (1991) Evidence for G-protein regulation of inward K^+ channel current in guard cells of fava bean. Plant Cell **3:** 1037–1044

Fairley-Grenot KA, Assmann SM (1992) Permeation of Ca^{2+} through K^+ channels in the plasma membrane of *Vicia faba* guard cells. J Membr Biol **128:** 103–113

Gratecos DE, Fisher H (1974) Adenosine 5′′-O(3-thiotriphosphate) in the control of phosphorylase activity. Biochem Biophys Res Commun **58:** 960–967

Hamill OP, Marty A, Neher E, Sakman B, Sigworth FJ (1981) Improved patch-clamp techniques for high resolution current recording from cells and cell-free membrane patches. Pflugers Arch **391:** 85–100

Hedrich RJ, Schroeder JI (1989) The physiology of ion channels and electrogenic pumps in higher plant cells. Annu Rev Plant Physiol **40:** 539–569

Hidaka H, Inagaki M, Kawamoto S, Sasaki Y (1984) Isoquinolinesulfonamides, novel and potent inhibitors of cyclic nucleotide-dependent protein kinase and protein kinase C. Biochemistry **23:** 5036–5041

Hille B (1992) Selective permeability: independence. *In* Ionic Channels of Excitable Membranes, Ed 2. Sinauer, Sunderland, MA, pp 337–361

Hodgkin AL, Huxley AF (1952) A quantitative description of membrane current and its application to conduction and excitation in nerve. J Physiol **117:** 500–544

Horn R (1991) Estimating the number of channels in patch recordings. Biophys J **60:** 433–439

Ilan N, Schwartz A, Moran N (1994) External pH effects on the depolarization-activated K channels in guard cell protoplasts of *Vicia faba*. J Gen Physiol **89:** 1184–1192

Inoue I (1981) Activation-inactivation of potassium channels and development of of the potassium channel spike in internally perfused squid giant axons. J Gen Physiol **78:** 43–61

Ivanina T, Perets T, Thornhill WB, Levin G, Dascal N, Lotan I (1994) Phosphorylation by protein kinase A of RCK1 K^+ channels expressed in *Xenopus* oocytes. Biochemistry **33:** 8786–8792

Ketchum KA, Joiner WJ, Sellers AJ, Kaczmarek LK, Goldstein SAN (1995) A new family of outwardly rectifying potassium channel proteins with two pore domains in tandem. Nature **376:** 690–695

Kim HY, Cote GG, Crain RC (1993) Potassium channels in *Samanea saman* protoplasts controlled by phytochrome and the biological clock. Science **260:** 960–962

Levitan IB (1994) Modulation of ion channels by protein phosphorylation and dephosphorylation. Annu Rev Physiol **56:** 193–212

Lewis CA (1979) Ion-concentration dependence of the reversal potential and the single channel conductance of ion channels at the frog neuromuscular junction. J Physiol **286:** 417–445

Li W, Luan S, Schreiber SL, Assmann SM (1994a) Evidence for protein phosphatase 1 and 2A regulation of K^+ channels in two types of leaf cells. Plant Physiol **106:** 963–970

Li W, Luan S, Schreiber SL, Assmann SM (1994b) Cyclic AMP stimulates K^+ channel activity in mesophyll cells of *Vicia faba* (L). Plant Physiol **106:** 957–961

Luan S, Li W, Rusnak F, Assmann SM, Schreiber SL (1993) Immunosuppressants implicate protein phosphatase regulation of K+ channels in guard cells. Proc Natl Acad Sci USA **90:** 2202–2206

Manor D, Moran N (1994) Modulation of small-conductance calcium-activated potassium channels in C6 glioma cells. J Membr Biol **140:** 69–79

Martiny-Baron G, Manolson MF, Poole RJ, Hecker D, Scherer GFE (1992) Proton transport and phosphorylation of tonoplast polypeptides from *Zucchini* are stimulated by the phospholipid platelet-activating factor. Plant Physiol **99:** 1635–1641

Moran N (1993) Depolarization-activated K channels in a plant motor cell are regulated by phosphorylation (abstract). Biophys J **64:** 387

Moran N (1994) Dual effect of phosphorylation on the depolarization-activated K channels in plasma membrane of *Samanea* motor cell protoplasts (abstract no. 529). Plant Physiol **105:** S-101

Moran N, Ehrenstein G, Iwasa K, Mischke C, Bare C, Satter RL (1988) Potassium channels in motor cells of *Samanea saman*: a patch-clamp study. Plant Physiol **88:** 643–648

Moran N, Fox D, Satter RL (1990) Interaction of the depolarization-activated K channel of *Samanea saman* with inorganic ions: a patch-clamp study. Plant Physiol **94:** 424–431

Noma A (1983) ATP-regulated K^+ channels in cardiac muscle. Nature **305:** 147–148

O'Rourke B, Backx PH, Marban E (1992) Phosphorylation-independent modulation of L-type calcium channels by magnesium-nucleotide complexes. Science **257:** 245–248

Pehtig R, Kuhn M, Payne R, Adler E, Chen T, Jaffe LF (1989) On the dissociation constants of BAPTA-type calcium buffers. Cell Calcium **10:** 491–498

Pickard BG (1973) Action potentials in higher plants. Bot Rev **39:** 172–201

Raz V, Fluhr R (1993) Ethylene signal is transduced via protein phosphorylation events in plants. Plant Cell **5:** 523–530

Roberts DM, Harmon AC (1992) Calcium-modulated proteins: targets of intracellular calcium signals in higher plants. Annu Rev Plant Physiol Mol Biol **43:** 375–414

Robinson RA, Stokes RH (1965) Electrolyte Solutions. Butterworths, London, p 571

Satter RL, Moran N (1988) Ionic channels in plant cell membranes. Physiol Plant **72:** 816–820

Satter RL, Morse MJ, Lee Y, Crain RC, Cote G, Moran N (1988) Light and clock-controlled leaflet movements in *Samanea saman*: a physiological, biophysical and biochemical analysis. Bot Acta **101:** 205–213

Schaller GE, Sussmann MR (1988) Phosphorylation of the plasma membrane H^+-ATPase of oat roots by a calcium-stimulated protein kinase. Planta **173:** 509–518

Schmidt C, Schelle I, Liao Y, Schroeder JI (1995) Strong regulation of slow anion channels and abscisic acid signaling in guard cells by phosphorylation and dephosphorylation events. Proc Natl Acad Sci USA **92:** 9535–9539

Schroeder JI, Ward JM, Gassmann W (1994) Perspectives on the physiology and structure of inward-rectifying K^+ channels in higher plants: biophysical implications for K^+ uptake. Annu Rev Biophys Biomol Struct **23:** 441–471

Shiina T, Wayne R, Lim-Tung HY, Tazawa M (1988) Possible involvement of protein phosphorylation/dephosphorylation in the modulation of Ca^{2+} channel in tonoplast-free cells of *Nitellopsis*. J Membr Biol **102:** 255–264

Sokal RR, Rohlf FJ (1981) Linear regression. *In* Biometry, Ed 2. WH Freeman, New York, pp 496–498

Spalding EP, Goldsmith MHM (1993) Activation of K^+ channels in the plasma membrane of *Arabidopsis* by ATP produced photosynthetically. Plant Cell **5:** 477–484

Stoeckel H, Takeda K (1993) Plasmalemmal, voltage-dependent ionic currents from excitable pulvinar motor cells of *Mimosa pudica*. J Membr Biol **131:** 179–192

Sussman MR (1992) Shaking *Arabidopsis thaliana*. Science **256:** 619

Sussman MR (1994) Molecular analysis of proteins in the plant plasma membrane. Annu Rev Plant Physiol Mol Biol **45:** 211–234

Thiel G, Blatt MR (1994) Phosphatase antagonist okadaic acid inhibits steady-state K^+ currents in guard cells of *Vicia faba*. Plant J **5:** 727–733

Ward JM, Pei Z, Schroeder JI (1995) Roles of ion channels in initiation of signal transduction in higher plants. Plant Cell **7:** 833–844

Wildon DC, Thain JF, Minchin PEH, Gubb IR, Reilly AJ, Skipper YD, Doherty HM, Donell PJ, Bowles DJ (1992) Electrical signalling and systemic proteinase inhibitor induction in the wounded plant. Nature **360:** 62–65

Winer BJ (1971) Design and analysis of single-factor experiment. *In* Statistical Principles in Experimental Design, Ed 2. McGraw-Hill, New York, pp 149–220

Wu W, Assmann SM (1995) Is ATP required for K^+ channel activation in *Vicia* guard cells? Plant Physiol **107:** 101–109

Zocchi G (1985) Phosphorylation-dephosphorylation of membrane protein controls the microsomal H^+-ATPase activity of corn roots. Plant Sci **40:** 153–159